International Journal of Mechanical, Industrial and Aerospace Sciences
ISSN: 2517-9950
Vol:7, No:11, 2013

Effects of Position and Cut-Out Lengths on the Axial Crushing Behavior of Aluminum Tubes: Experimental and Simulation

B. Käfer, V. K. Bheemineni, H. Lammer, M. Kotnik, F. O. Riemelmoser

***Abstract*—**Axial compression tests are performed on circular tubes made of Aluminum EN AW 6060 (AlMgSi0.5 alloy) in T66 state. All the received tubes have the uniform outer diameter of 40mm and thickness of 1.5mm. Two different lengths 100mm and 200mm are used in the analysis. After performing compression tests on the uniform tube, important crashworthy parameters like peak force, average force, crush efficiency and energy absorption are measured. The present paper has given importance to increase the percentage of crush efficiency without decreasing the value energy absorption of a tube, so a circumferential notch was introduced on the top section of the tube. The effects of position and cut-out lengths of a circumferential notch on the crush efficiency are well explained with relative deformation modes and force-displacement curves. The numerical simulations were carried on the software tool ANSYS/LS-DYNA. It is seen that the numerical results are reasonably good in agreement with the experimental results.

***Keywords*—**Crash box, Notch triggering, Energy absorption, FEM simulation.

I. INTRODUCTION

CURRENTLY, the most important objective of automotive industries is to design light weight vehicles in order to be environment-friendly. It is important for such vehicles to meet the safety requirements during collisions. Crashworthiness is concerned with the absorption of crash energy through controlled failure mechanism. Researchers and designers of crashworthy systems have intensively tested and analyzed the axial crushing of tubes due to their qualitative characteristics as impact energy absorption elements called as crash boxes.

Metallic tubes are subjected to axial crushing to achieve energy absorption due to their plastic deformation. Alexander [1] in 1960 conducted the axial crushing on metallic circular shells. From then during the last 5 decades a lot of theoretical, experimental and numerical investigations were done on thin walled tubes of various dimensions, cross sections and materials under static and dynamic axial loadings. Different types of impact energy absorbers which absorb energy through their plastic deformation are well reviewed in [2]. Short uniform round tubes in axial compression may collapse in axi-symmetric mode, non-symmetric mode, mixed mode depending on diameter, thickness and length of the tube [3], [4].

B. Käfer, V. K. Bheemineni, and F. O. Riemelmoser are with the Carinthia University of Applied Sciences, Mechanical engineering, Villach, 9500 Austria (e-mail: Bernd.Kaefer@edu.fh-kaernten.ac.at, V.Bheemineni@fh-kaernten.at, F.Riemelmoser@fh-kaernten.at).

H. Lammer is with the W3C Wood Carinthian Competence Center, St. Veit, 9300 Austria (e-mail: h.lammer@kplus-wood.at).

M. Kotnik is with the Oprema Ravne, Ravne na Koroskem, 2390 Slovenia (e-mail: Marjan.Kotnik@opremaravne.si).

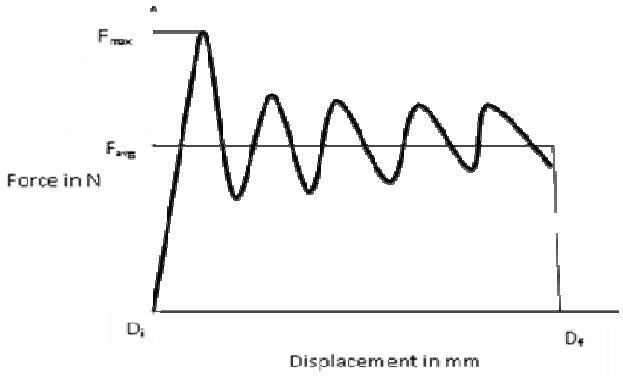

Fig. 1 Assumed force-displacement curve of a progressively crushed metallic tube

The assumed schematic force-displacement curve of a progressively crushed uniform metallic tube is shown in Fig. 1, where 'F_{max}' is the maximum force, 'F_{avg}' is the average force, 'D_i' is initial crush displacement and 'D_f' is the final crush displacement. Then the total energy absorbed by the tube can be calculated by multiplying the average force with the final crush displacement. The crush efficiency is the ratio of average force to the maximum force in percentage. In the present analysis attempts are made to increase the crush efficiency of the tubes by introducing a circumferential notch at the approximate position where first plastic hinge took place during compression. During compression of the notched samples, the circumferential notch is expected to decrease the magnitude of the first peak force. One circumferential notch per one sample is used in order to achieve approximately same energy absorption as of a crushed uniform tube. The effects of position and cut-outlengths of the crushed circumferential notched tubes on the energy absorption and crush efficiency are explained and compared.

For reducing the experimental costs and time consumption, finite element simulations are used as a powerful tool for solving most complex problems associated with crash. A lot of numerical investigations were found on energy absorbers in the literature. Most of them investigated the behavior of uniform metallic tubes which are collapsed by folding progressively [5] due to compression between two flat plates

and small number of investigations was present focusing on tube internal inversion [6], tube external inversion [7] and axial tearing of metallic tubes [8] using angled dies. In the paper the numerical simulations are focused to obtain the force-displacement curves using finite element modeled circumferential notched tubes and compared with the experimental force-displacement curves. The software ANSYS/LS-DYNA [9] was used in this research, where the numerical modeling was developed using the ANSYS-preprocessor and later written as transient nonlinear explicit code LS-DYNA (.k) file for obtaining the deformed modes and force-displacement graphs.

II. Experimental Setup

The quasi-static experimental setup comprising of uniform and circumferential notched aluminum tubes and crush plates as shown in Fig. 1. The Aluminum EN AW 6060 (AlMgSi0.5 alloy) tubes are received in T66 state. The tubes have an outer diameter of 40mmand a thickness of 1.5mm. Initially a length of 100mm is considered while analyzing the effect of position and cutout lengths on the axial crushing behavior of aluminum tubes. After selecting the best sample which gives us the high crush efficiency, that sample's behavior (crush efficiency) was tested under compression by increasing its length from 100mm to 200mm. The experiments are performed on the Test® compression machine of 250 kN capacity and all the 100mm length samples are crushed to 50% of their lengths with a quasi-static velocity of 10mm/min.

TABLE I
Selected Values of Position and Cut-Out Lengths for the Notched Samples

Sample No.	A (mm)	B (mm)	C (mm)
ENS1	4	0.4	5
ENS2	5	0.5	5
ENS3	6	0.6	5
ENS4	7	0.7	5
ENS5	7	0.7	6
ENS6	7	0.7	7
ENS7	7	0.7	8
ENS8	7	0.7	9
ENS9	7	0.7	10

Fig. 2 shows the schematic representation of circumferential notch on the wall of a tube with thickness 't' equal to 1.5mm. 'A' is the length of the notch size, 'B' is the length of position of notch center from the top the tube and 'C' is the maximum cut-out length on the tube's wall. The values of 'A','B' and 'C' used for each experimental notches sample (ENS)with in the analysis are tabulated in Table I.

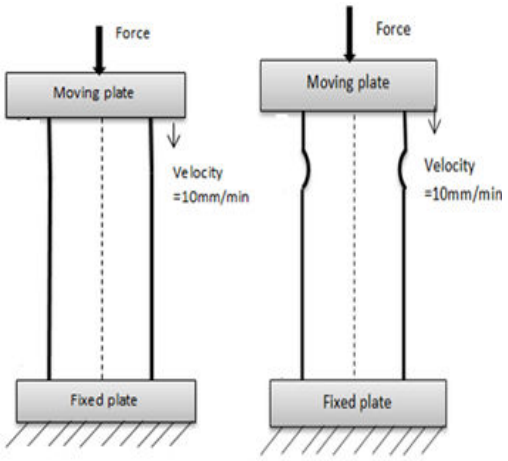

(a) (b)

Fig. 1 Quasi-static experimental setup (a) 2D front view of uniform tube under compression (b) 2D front view of circumferential notched tube under compression

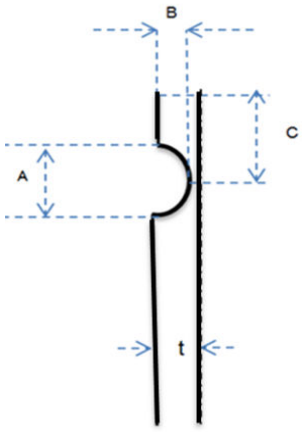

Fig. 2 D Schematic representation of circumferential notched tube wall

III. Numerical Modeling

The software tool ANSYS/LS-DYNA [9] features all the capabilities that are necessary for modeling a system with the characteristics of the given problem. The numerical modeling is classified into four steps as follows.

A. Element Type

For modeling metallic tube and crush plates, an element type 'Shell 163' (an explicit thin shell) was used. This element type has 4 nodes with 12 degrees of freedom at each node (i.e., translations, rotations, accelerations and velocities in X, Y and Z directions). "Belytschko-Tsay" fully integrated element formulation was used in order to eliminate the hour glassing problems that are likely to occur when large deformations took place. Three integrated points through the thickness of element was chosen throughout our analysis because the given problem is based on nonlinear analysis.

B. Material Modeling and Meshing

TABLE II
MATERIAL PROPERTIES OF ALUMINUM AND RIGID MATERIALS

Material Properties	Rigid	Al-6060(T66)
Density (kg/m^3)	7600	2800
Young's Modulus (Pa)	210e9	69e9
Poisson's Ratio	0.3	0.3
Yeild strength (Pa)	-	206e6
Tangent modulus (Pa)	-	320e6

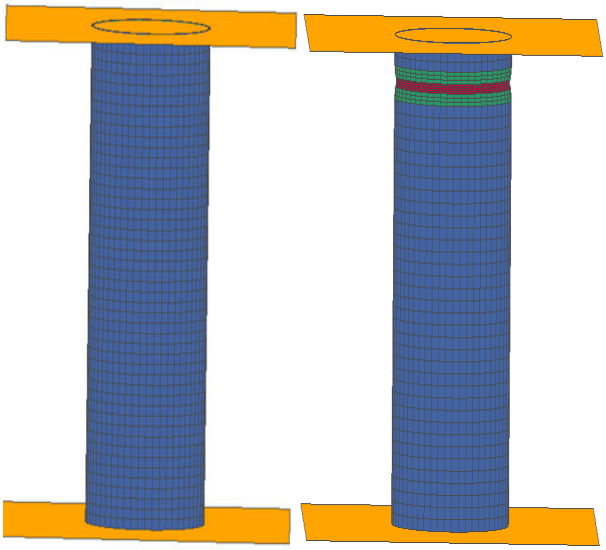

(a) (b)

Fig. 3 Geometric model of (a) Uniform tube (b) Notched tube

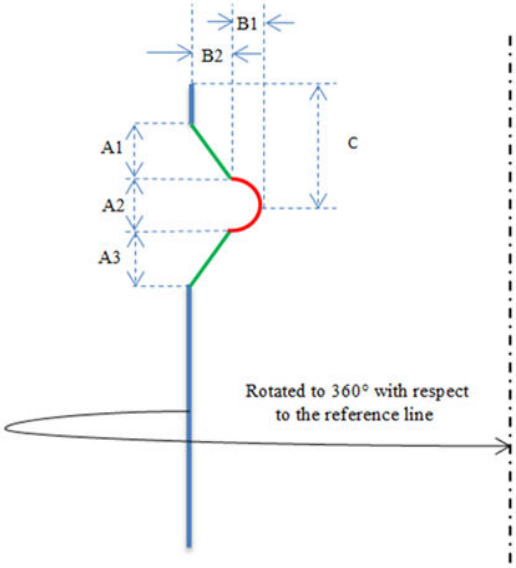

Fig. 4 Considered initial steps while modeling the notched tube

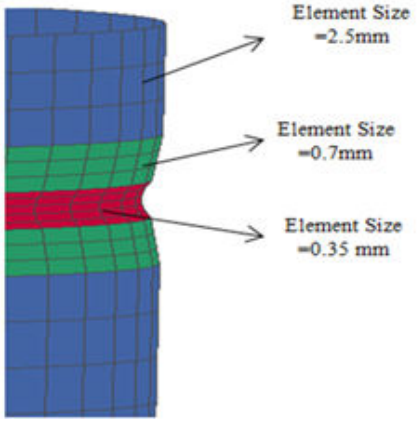

Fig. 5 Meshing of notched tube with selective element size for the areas differentiated by colors

The aluminum tube was modeled with strain rate independent inelastic bilinear isotropic hardening material law. The material properties thus required for material modeling of aluminum tube is given in Table II. For modeling top and bottom plates, the material model 'Rigid' was chosen. The advantage of choosing `Rigid` model is that they do not show any deformation and there will be a significant reduction of solution time. Although the rigid materials are not subject to deformation, realistic values for the material properties must be defined [10]. The steel material properties are used for modeling rigid body as given in Table II.

The geometries of uniform and notched tubes are modeled by considering the dimensions of the tubes used in the experiments. While dealing with the shell elements, the geometry should be modeled as surface areas, and the geometry thickness can be defined using real constants of an element in ANSYS preprocessor. The surface area of the uniform tube is meshed uniformly with an element size of 2.5mm. The initial steps followed while modeling the notch for a tube is shown in Fig. 4. Key points are selected on the ANSYS XY workplane according to the X, Y coordinates A1, A2, A3, B1, B2 and C whose values for each simulated notched sample (SNS) are listed in Table III. Note that the sum of the values A1, A2 and A3 is equal to the experimental samples length of the notch size 'A' and the sum of the values B1 and B2 is equal to the experimental samples notch cut-out length 'B'. Through the Keypoints the notch of a tube was modeled by using two straight lines which in turn connected by an arc shown in green and red colors in Fig. 4. The whole tube can be modeled by rotating the connected lines and arc by 360° with respect reference line which is at a distance equal to the radius of the tube. The modeled tube is shown in Fig. 3 (b) with three areas differentiated with the colors blue, green and red. While meshing, the element sizes used for each of the areas are shown in Fig. 5, the assigned thicknesses at each area with respect to varied samples are listed in Table IV clearly by representing colors. The top moving plate and bottom fixed plate are modeled with single shell element, hence no meshing is required.

TABLE III
LENGTHS USED FOR MODELING NOTCHED SAMPLES IN SIMULATIONS

Sample No.	A1=A2=A3 (mm)	B1=B2 (mm)	C (mm)
SNS1	1.33	0.2	5
SNS2	1.66	0.25	5
SNS3	2	0.3	5
SNS4	2.33	0.35	5
SNS5	2.33	0.35	6
SNS6	2.33	0.35	7
SNS7	2.33	0.35	8
SNS8	2.33	0.35	9
SNS9	2.33	0.35	10

TABLE IV
ASSIGNED THICKNESS FOR THE SELECTED COLORS SHOWN IN FIG. 5

Sample No.	Thickness assigned to the elements in color (mm)		
	Blue	Green	Red
SNS1	1.5	1.3	1.1
SNS2	1.5	1.25	1
SNS3	1.5	1.2	0.9
SNS4	1.5	1.15	0.8
SNS5	1.5	1.15	0.8
SNS6	1.5	1.15	0.8
SNS7	1.5	1.15	0.8
SNS8	1.5	1.15	0.8
SNS9	1.5	1.15	0.8

C. Loading and Boundary Conditions

In transient analysis the loads must be defined in terms of time. Two array parameters "TIME" and "VELOCITY" are used. Under array parameter "TIME" we used the 1x2 array for setting the start time to zero and the solution end time to two seconds. Under array parameter "VELOCITY", the velocity of the moving plate was defined. The velocity of 25mm/s is considered, so the total crushing displacement will be 50mm in 2 seconds. The rigid body has six degrees of freedom (i.e. rotations and translations in x, y, z directions). The moving plate is supposed to move in negative Z-direction axial to the tube, and constrained to all other translations and rotations. The bottom plate is constrained to all rotations and translations.

D. Contact Definitions

After creating three parts (one tube and two rigid plates), the contacts between them have to be defined. A'NODE-TO_SURFACE' contact was used between plates and tube with a static friction coefficient of 0.3. Using this contact algorithm the reaction forces at the tube plate interface will be extracted.

After modeling the system with the above steps the ANSYS (.DB) file was written or converted to LS-DYNA keyword (.k) file, where the inelastic rate independent isotropic hardened material aluminum was automatically transferred to 'Plastic Kinematic', material model 3 in LS-DYNA. In the material card β=1 indicates the material is isotropic hardened, β=0 indicates the material has kinematic hardened behavior.

IV. EXPERIMENTAL RESULTS

A. Effect of Cut-Out Lengths

Fig. 6 shows the comparison of force-displacement curves from experimentally crushed uniform and notched tubes. The experimental notched samples has a notch positioned constant at 5mm from the top of a tube and with varied cut-out lengthsin incremental order from 0.4mm for ENS1 to 0.7mm for ENS4. From the curves the important crashworthy parameters are extracted and tabulated in Table V. The results showed that the uniform tube showed higher average force and energy absorption than the notched samples. However its crush efficiency is somewhat lesser than ENS2, ENS3 and ENS4 because of high peak force. From notched tubes, ENS3 and ENS4 showed good results of energy absorption and crush efficiency. ENS4 showed 3.8% higher energy absorption and 4.5% lesser crush efficiency than ENS3.By looking at the Fig. 6 and Table V, the maximum force was observed at the first peak for the uniform tube and notched samples ENS1, ENS2 and ENS3, where for the ENS4 the maximum force was observed at the last peak. With the advantage of absorbing higher energy than the other notched samples, ENS4 has been selected for the further investigations i.e., varying the position of the notch.

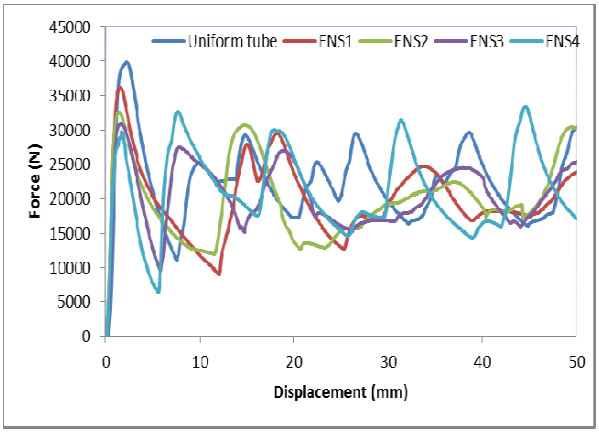

Fig. 6 Force-displacement curves of the unifom and notched samples with varied cut-out lengths

TABLE V
COLLECTED DATA FROM THE CRUSHED NOTCHED SAMPLES WITH VARIED CUT-OUT LENGTHS

Sample No.	Maximum Peak force (kN)	Average force (kN)	Energy absorbed (J)	Crush efficiency (%)
Uniform tube	39.8	22.4	1120	56.4%
ENS1	36.1	19.8	991.6	54.8
ENS2	32.5	19.6	983.1	60.4
ENS3	30.8	20.4	1023.6	66.3
ENS4	33.5	21.2	1064.7	63.4

B. Effect of Positions

Fig. 7 show the compared force-displacement curves of the notched samples having constant cut-out length of 0.7mm with varied notch position lengths with incremental order from

5mm for ENS4 to 10mm for ENS9.The collected data from the curves is listed in the Table VI. After increasing the length of the notch position, all the samples showed higher energy absorption than ENS4. ENS5 and ENS6 failed to reach the crush efficiency of ENS4 because of their maximum forces at the second peak. ENS8 showed high energy absorption with a very good crush efficiency of 72.9%. Of all the notched samples ENS9 showed high crush efficiency of 74.2%, and less peak force of 30.7 kN with an energy absorption of 1.8% higher than the of the uniform tube.

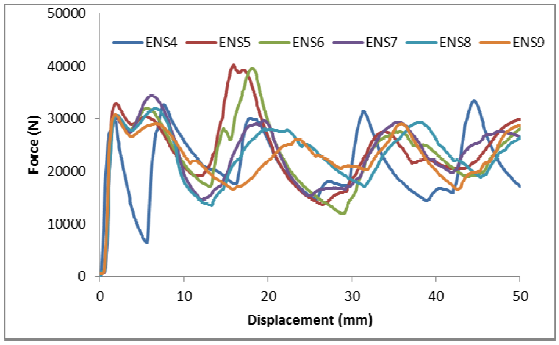

Fig. 7 Force-displacement curves of the notched samples with varied positions

TABLE VI
COLLECTED DATA FROM THE CRUSHED NOTCHED SAMPLES WITH VARIED POSITIONS

Sample No.	Maximum Peak force (kN)	Average force (kN)	Energy absorbed (J)	Crush efficiency (%)
ENS4	33.5	21.2	1064.7	63.4
ENS5	40.1	23.9	1195.1	59.6
ENS6	39.4	23.6	1181.8	59.8
ENS7	34.3	23.1	1159.8	67.6
ENS8	31.9	23.9	1195.1	72.9
ENS9	30.7	22.8	1141.3	74.2

C. Effect of Tube's Length

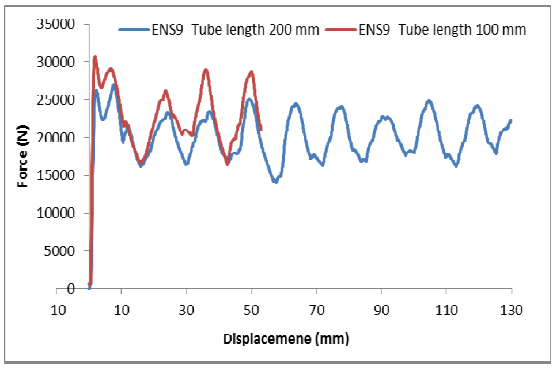

Fig. 8 Force-displacement curves of the crushed ENS9 with varied tube lengths

TABLE VII
COLLECTED DATA FROM THE CRUSHED ENS9 WITH VARIED TUBE LENGTHS

Sample No.	Maximum Peak force (kN)	Average force (kN)	Crush efficiency (%)
ENS9-Tube length=200mm	27	20.1	74.7
ENS9 Tube length=100mm	30.7	22.8	74.2

Fig. 8 show the compared force-displacement curves of ENS9 where the initial lengths of the tubes before crushing are 100mm and 200mm. The 100mm sample if crushed till 50mm and 200mm sample crushed till the maximum possible130mm. Because of two crushed displacements, their absorbed energies are not compared; however the maximum peak forces, average forces and crush efficiencies are compared given in the Table VII. The comparisons showed that maximum peak force and the average force decreases as the length of the tube increases still maintaining the similar crush efficiency.

D. Deformation Modes

The deformation modes of the crushed notched samples with varied cut-out lengths are shown in Fig. 9, with varied positions are shown in Fig. 10. The samples ENS1, ENS2 and ENS3 folded in the mixed mode with one circular axi-symmetric fold and followed by non-symmetrical folds. For these samples during the formation of first axi-symmetric folding the top edge of the tube faces the inwards with respect to the tube mean diameter. For ENS4 the top portion of the tube stretches and the top edge faced outwards with respect to the tube mean diameter. From then it starts crushing with repetitive axi-symmetric folding's. That is why its peak forces increases with increased number of peaks as observed in Fig. 6. After fixing the cut-out length to 0.7mm, while increasing the positions of the notch, for ENS9 it is observed that the first fold formed with 3 sections of the top edge facing inwards and 3 sections of the top edge facing outwards with respect to the mean diameter as shown in Fig. 10 (e). This behavior forces the rest of the tube to deform in a repetitive 3 lobe diamond folding shape. Fig. 11 shows the clear vision of observed 3 lobe diamond folding of a 130mm crushed ENS9, whose tube length before crushing is 200mm.

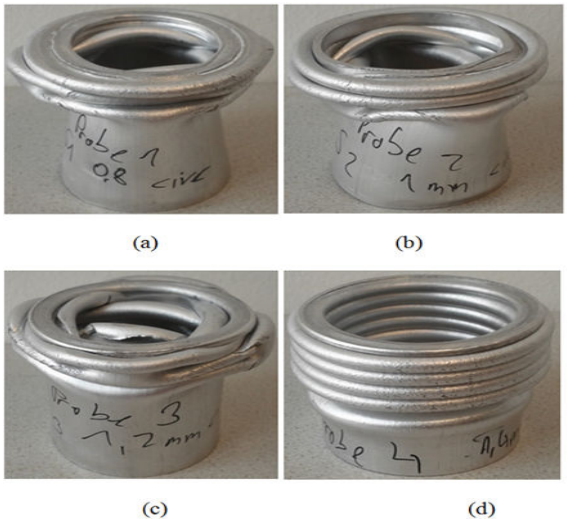

Fig. 9 Deformation modes of (a) ENS1 (b) ENS2 (c) ENS3 and (d) ENS4

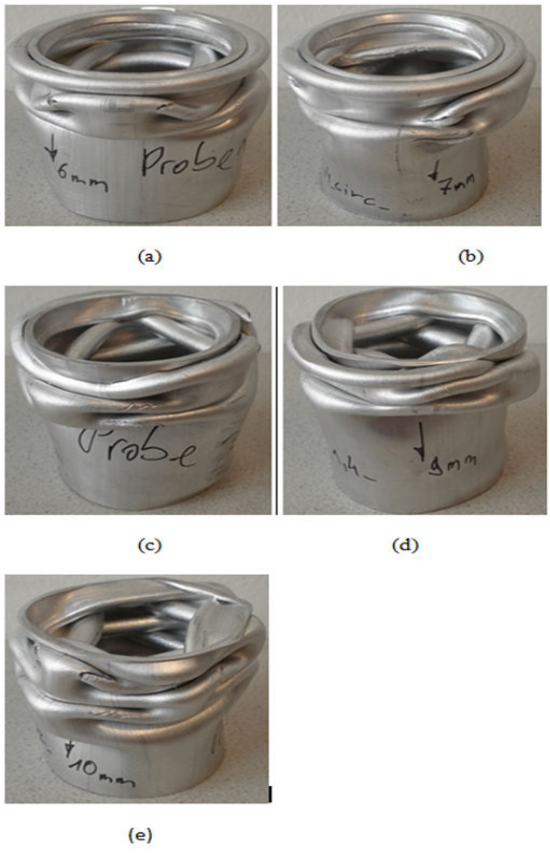

Fig. 10 Deformation modes of (a) ENS5 (b) ENS6 (c) ENS7 (d) ENS8 and (e) ENS9

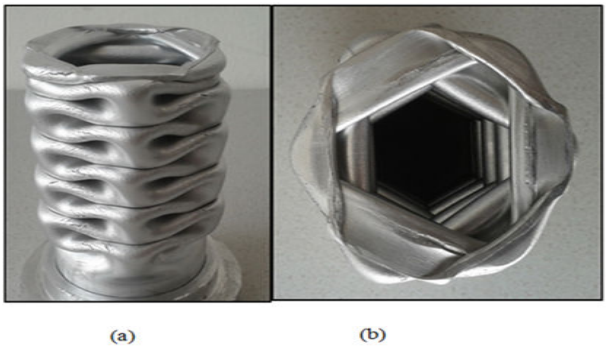

Fig. 11 Deformation modes of ENS9 of tube length 200m (a) front view (b) Top view

V. Simulations Results and Comparison

The deformation modes of SNS4 at different crush lengths are shown in Fig. 12. It is observed that during compression the initial bending moment occurs at the center region of the notch and the whole area of the notch will be crushed at 7mm as shown in Fig. 12 (b). After that the top section of the tube stretches and bends with the top edge facing the outwards of the tube as shown in Fig. 12 (c). From then the rest of tube crushes by forming circular axi-symmetric folds till the final crush displacement of 50mm like as shown in the Fig. 12 (d). All the samples in the simulations crushed with the similar behavior; however during experiments only ENS4 showed this type of crushing behavior.

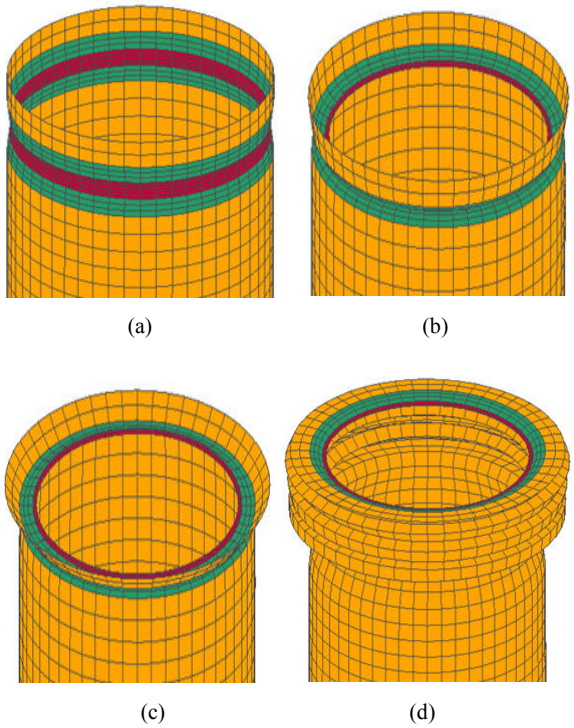

Fig. 12 Deformation modes of SNS4 at crushed lengths of (a) 0mm (b) 7mm (c) 9mm and (d) 50mm

The force-displacement curves of the notched samples obtained from the simulations are compared separately with the experimental samples as shown in the Fig. 13. The comparisons showed similar first peak forces from both experimental and simulated curves. After the first peak the variations in force with displacement depends on the type deformation mode in which the tube crushes. During simulations all the samples are crushed with circular axi-symmetric behavior, where the experimental tubes crushed in 3 different deformation modes like mixed, 3-lobe diamond and circular axi-symmetric. Of all the experimental samples the circular axi-symmetric behavior was shown by only ENS4. So the ENS4 and SNS4 showed the similar behavior of variations in force till the end of crush displacement as shown in Fig. 13 (d).

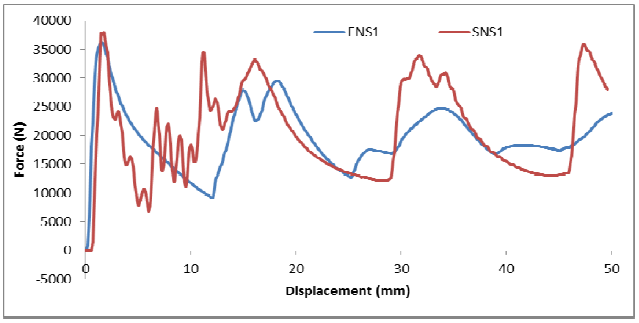

(a)

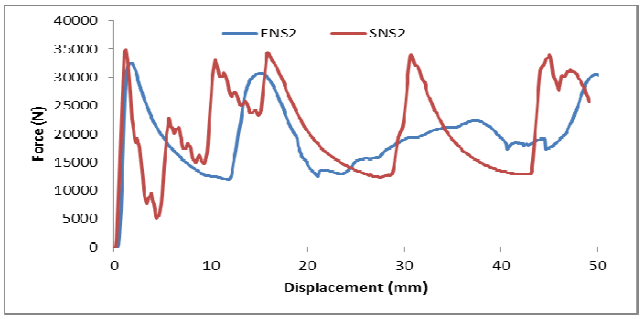

(b)

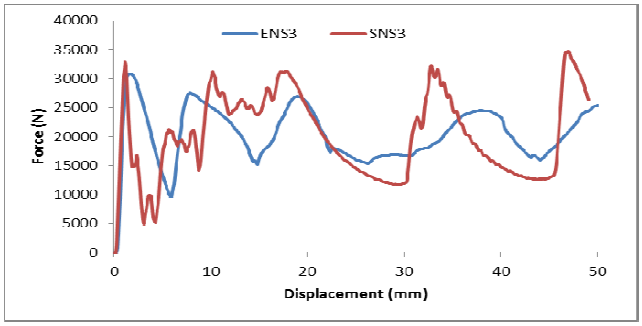

(c)

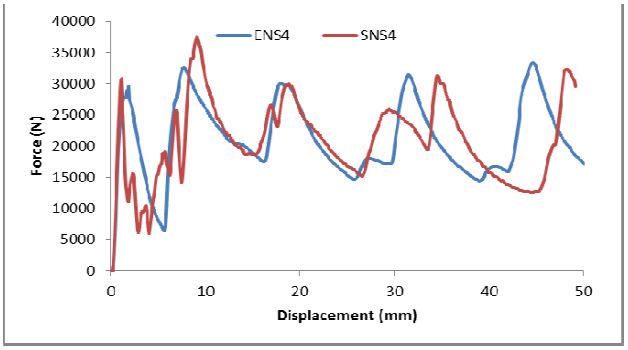

(d)

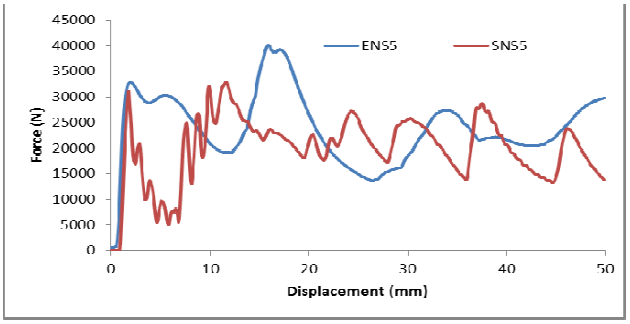

(e)

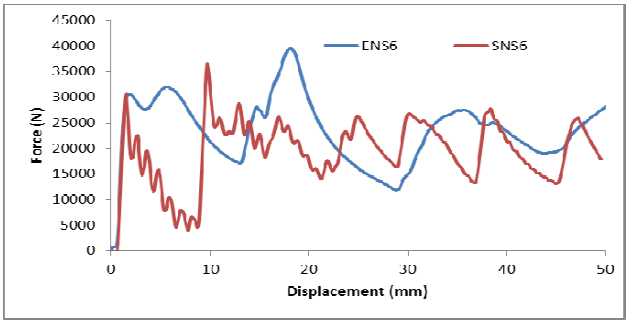

(f)

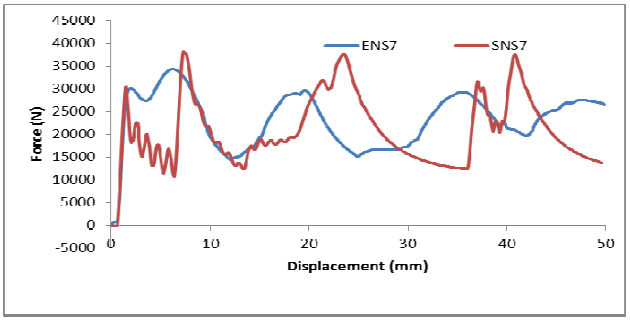

(g)

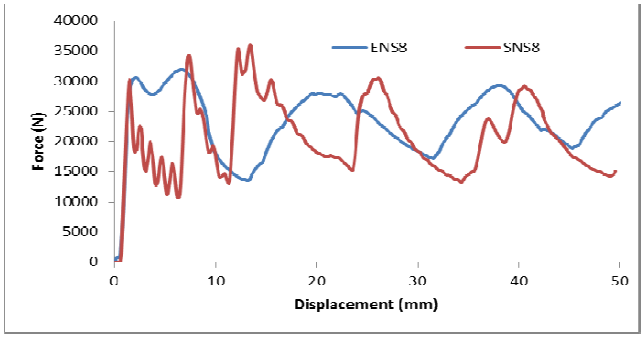

(h)

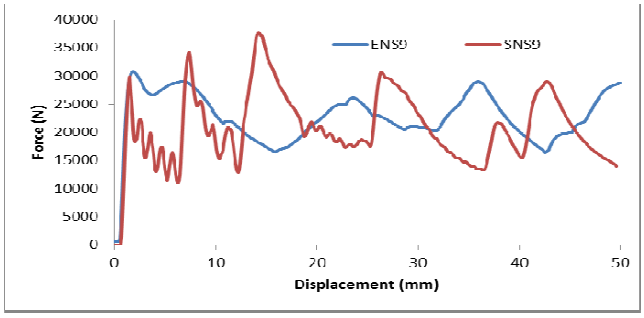

(i)

Fig. 13 Comparison of force-displacement curves of simulated notched samples with (a) ENS1 (b) ENS2 (c) ENS3 (d) ENS4 (e) ENS5 (f) ENS6 (g) ENS7 (h) ENS8 (i) ENS9

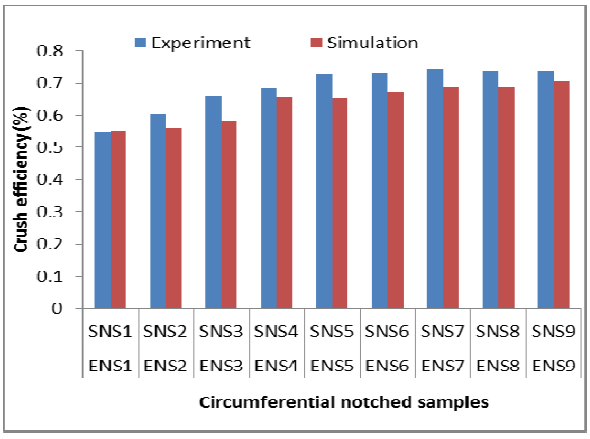

Fig. 14 Experimental and numerical comparisons of the crushed notched samples

Even though the crushing behavior of the samples differs, the observed differences in the magnitude of experimental and simulated average forces are small. During simulations due to the circular axi-symmetric mode of deformation, for the most of the samples, the maximum forces are observed on the peaks later to the first one. So here in the section of comparison of experimental and simulated results, the crush efficiency percentage was calculated by dividing the samples total average force with its first peak force. Fig. 14 shows the comparison experimental and simulated notched samples crush efficiencies. The comparisons showed that for both the experimental and simulated samples, the crush efficiency increases with the increase in the sample's number.

VI. Conclusion

The effects of position and cut-out lengths on the axial crushing behavior of the circumferential notched aluminum tubes are investigated experimentally and numerically. In the experiments, mixed mode deformation is observed while investigating the effect of cut-out lengths. When the lengths of the notch position increased the samples changed their deformation mode from mixed to 3-lobe diamond folding. The samples crushed with 3-lobe diamond folds showed high crush efficiency and absorbed the same amount of energy as of a crushed uniform tube did. The numerical investigations are carried on ANSYS/LS-DYNA. The simulated results showed that they are reasonably good in agreement with the experimental results. In simulation all the samples are crushed by forming circular axi-symmetric folds. In order to observe the effect of deformation modes like mixed mode or 3 lobe-diamond folding's on the force-displacement curves from the crushed simulated samples, there is a need to investigate the present analysis by modeling some imperfections on the tube's geometry.

References

[1] Alexander JM, "An Approximate Analysis of the Collapse of Thin Cylindrical Shells under Axial Loading". Quarterly Journal. of Mechanics & Applied Maths,1960
[2] Alghamdi AAA, "Collapsible impact energy absorbers: an overview", in The Journal of Thin-Walled Structures, vol 39, No.2, 2001, pp.189–213
[3] Andrews, K. R. F., England, G. L. & Ghani, E. "Classification of the axial collapse of cylindrical tubes under quasi-static loading". International Journal of Mechanical Sciences, 1983
[4] S.R. Guillow, G. Lu, R.H. Grzebieta. "Quasi-static axial compression of thin-walled circular aluminium tubes"; International Journal of Mechanical Sciences, 2001
[5] H. R. Zarei, M. Kröger, "Multiobjective crashworthiness optimization of circular aluminum tubes", In The Journal of Thin-Walled Structures, vol 41, No.3, 2006, pp. 301–308
[6] P.A.R. Rosa, J.M.C. Rodriques, P.A.F Martins, "External inversion of thin-walled tubes using a die: experimental and theoretical investigation", in The International Journal of Machine Tools & Manufacture, vol 43, No.8, 2003, pp.787-796
[7] P.A.R. Rosa, J.M.C. Rodriques, P.A.F Martins, "Internal inversion of thin-walled tubes using a die: experimental and theoretical investigation", in The International Journal of Machine Tools & Manufacture, vol 44, No.7-8, 2004, pp.775-784
[8] V. K. Bheemineni, B. Käfer, H. Lammer, M. Kotnik, and F. O. Riemelmoser," Energy Absorption and Axial Tearing Behaviour of Metallic Tubes Using Angled Dies: Experimental and Numerical Simulation" in The World Academy of Science, Engineering and Technology, 79, 2013,pp-625-629
[9] ANSYS/LS-DYNA user's guide 2009. ANSYS Inc., USA
[10] Frank Ratter, Dennis Lueddeke, Shyh-Chour Huang, "Finite Element Analysis of the Lateral Crushing Behavior of Segmented Composite Tubes"; in The Journal of Engineering Technology and Education, vol 6, No.1, 2009, pp.1-16